Annals of Nuclear Cardiology Vol. 5 No. 1 95–100

REVIEW ARTICLE

Cardiac PET: Interventional Physiology to Guide PCI

Nils P. Johnson, MD, MS

Received: July 23, 2018/Revised manuscript received: August 18, 2018/Accepted: September 5, 2018
J-STAGE advance published: May 10, 2019

Abstract

Currently most stable patients referred for invasive angiography do not have obstructive disease, implying an enormous opportunity to avoid unnecessary, invasive, and expensive procedures. Cardiac positron emission tomography (PET) offers a robust and non-invasive tool for quantifying absolute blood flow as a "gatekeeper" to cardiac catheterization. It images the entire left ventricle down to branch vessels, permitting a "physiologic angiogram" while normalizing flow values for the amount of supplied myocardium. Flow imaging has been demonstrated to be accurate compared to invasive measurements, precise to 20% on test/retest assessment, and routinely achievable in >99% of daily clinical cases. Coronary flow capacity (CFC) integrates both resting and hyperemic flow together along the continuum from infarction to ischemia to normal levels. CFC predicts prognosis and identifies which patients benefit from revascularization. Emerging work allows cardiac PET to make an assessment of subendocardial hypoperfusion, relevant since this layer of the myocardium suffers "first and worst" from epicardial disease. A case example highlights many of the aspects of cardiac PET described in this review article.

Keywords: Absolute flow quantification, Coronary revascularization, Positron emission tomography
Ann Nucl Cardiol 2019; 5 (1): 95–100

Almost 70 years have passed since the first *in vivo* measurements of myocardial blood flow in humans (1). Since its development beginning with an animal model in 1979 (2) and humans in 1982 (3), cardiac positron emission tomography (PET) has established itself as the reference standard for quantitative perfusion imaging. Published results from approximately 15,000 subjects in 250 manuscripts (4) support its numerous, daily use around the world for patient care. At our own center in Houston, Texas, we began routine flow assessment in April 2007 for every rest/stress perfusion case, now exceeding 6,200 patients and research subjects.

The lessons learned from our past decade of flow quantification provide key insights into addressing an urgent clinical need: appropriately selecting patients for invasive angiography and revascularization. In the United States, almost two-thirds of stable patients referred for invasive angiography did not have obstructive disease (5), implying an enormous opportunity to avoid unnecessary, invasive, and expensive procedures. While stable patients with symptoms referred directly for invasive angiography had a higher prevalence of obstructive lesions at catheterization than those first referred for non-invasive testing (27% versus 6%) in the PLATFORM trial (6), revascularizable disease remained a distinct minority in both populations. Hence while "clinical judgment" increases the pre-test probability of finding important coronary disease, non-invasive imaging could significantly refine referrals to the catheterization laboratory. Notably, a recent analysis of national statistics in America showed that the volume of non-acute PCI consistently fell every year from 2010 to 2014, down by 34% over that period (7) and probably multifactorial in nature.

Current reimbursement for percutaneous coronary intervention (PCI) in the United States demands that 3 requirements be met (8). First, the lesion has to be feasible for percutaneous treatment, which is almost never a limitation in the modern era. Second, clinical symptoms of angina must remain despite optimal medical therapy. Third, objective evidence of myocardial ischemia needs to be provided, although a specific

doi: 10.17996/anc.19-00085

Weatherhead PET Center, Division of Cardiology, Department of Medicine, McGovern Medical School at UTHealth and Memorial Hermann Hospital, Houston, Texas.

Table 1 Absolute myocardial flow thresholds

Rest flow (cc/min/gm)	Stress flow (cc/min/gm)	CFR	Other features	Interpretation
<0.2			Q-waves Wall motion abnormality	Transmural scar or hibernation
	<0.83	<1.27	ST-segment depression Vasodilator-induced angina Stress-induced uptake defect	Frank ischemia
	<1.09	<1.60	Some of above features	Moderate ischemia or borderzone
	<2.17	<2.90		Typical flows with risk factors or mild CAD
	>2.17	>2.90		Normal flows (healthy volunteers)

test is not specified. National data from a large, contemporary, cardiac imaging registry of over 1,700 patients shows that the most common preceding modality was single photon emission computed tomography (9).

This review addresses the ability of cardiac PET to quantify absolute blood flow in order to separate the minority of patients who need an invasive procedure from the majority who require only medical therapy.

Clinical requirements

In order to satisfy clinical needs, any non-invasive tool to quantify myocardial blood flow should meet several requirements. First, it must image the entire left ventricle in order to define the physiology down to branch vessels. Over 15 years ago we developed an anatomic atlas for cardiac PET based on angiographic correlations from almost 900 subjects (10), permitting a "physiologic angiogram" before entering the catheterization laboratory. Second, and relatedly, flow must be provided for small regions of the left ventricle, not only average global flow alone. While global stress flow and absolute flow reserve have proven to be strong predictors of prognosis on a population basis, these blunt averages can mask important regional disease that explains clinical symptoms, changes medical management, or would be appropriate for revascularization in individual patients. Third, flow quantification must account for the amount of distal myocardium by normalizing absolute flow (cc/min) to supplied tissue mass (g). As noted over 20 years ago, "absolute flow, expressed in ml/min is meaningless because the myocardial distribution to be perfused is unknown and varies widely between different arteries and different subjects" (11).

Fourth, the model for converting perfusion into flow must be accurate, precise, and robust. Our retention model, validated invasively against electromagnetic flow meters in an animal model (12), requires only an early arterial input image (for example, the first 2 minutes beginning immediately upon injection of ^{82}rubidium) and a late myocardial image (next 5 minutes after the arterial phase). Repeated cardiac PET imaging on the same day shows that flow varies by 10% in stable subjects mainly due to the technique itself, rising to 20% a few days apart due to combined biologic plus methodologic variability (13). Others have reported that our "retention approach yielded a better agreement with microsphere flow" and that the "retention approach is more robust" (14), probably because it avoids fitting noisy time-activity curves. During 11 years of routine clinical use at our center, <1% of rest/stress perfusion cases did not produce valid flow results, typically due to scanner failure or unanticipated anomalous venous anatomy.

Routine flow quantification demands additional processing time compared to relative uptake imaging. In our own center, we developed software that reduces this time to a minimum－generally a few minutes and similar to quantifying ejection fraction. Once arterial input selection has been automated, the required time will fall further.

Some centers have started to explore dynamic single photon emission computed tomography (SPECT) for absolute flow quantification (15, 16). However, this data currently exists only for small series (<50 subjects) at the global left ventricular or major epicardial territory level, unlike the vast series (15,000 subjects) for cardiac PET (4) able to resolve flow down to branch vessels (10). Additionally, paired comparisons of dynamic SPECT to cardiac PET show wide 95% imprecision for global absolute flow of -1.1 to +1.7 cc/min/gm (15) or -0.6 to +0.6 cc/min/gm (16) and for global flow reserve of -0.9 to +1.3 (15) or -0.6 to +0.5 (16).

Interpreting absolute myocardial flow

Regardless of the technique used to measure normalized absolute flow, we must interpret its value for clinical application as summarized in the Table 1. Two extremes exist along the flow spectrum. At the lowest end, absolute flow and flow reserve fall to levels that cause frank ischemia during hyperemia. At the highest end we observe flow values typical in normal people (not patients). Prior work by our group enrolled over 120 volunteers screened rigorously for occult or undisclosed risk factors (coronary calcium, serum lipids, abnormal electrocardiogram, vital signs, and clinical and

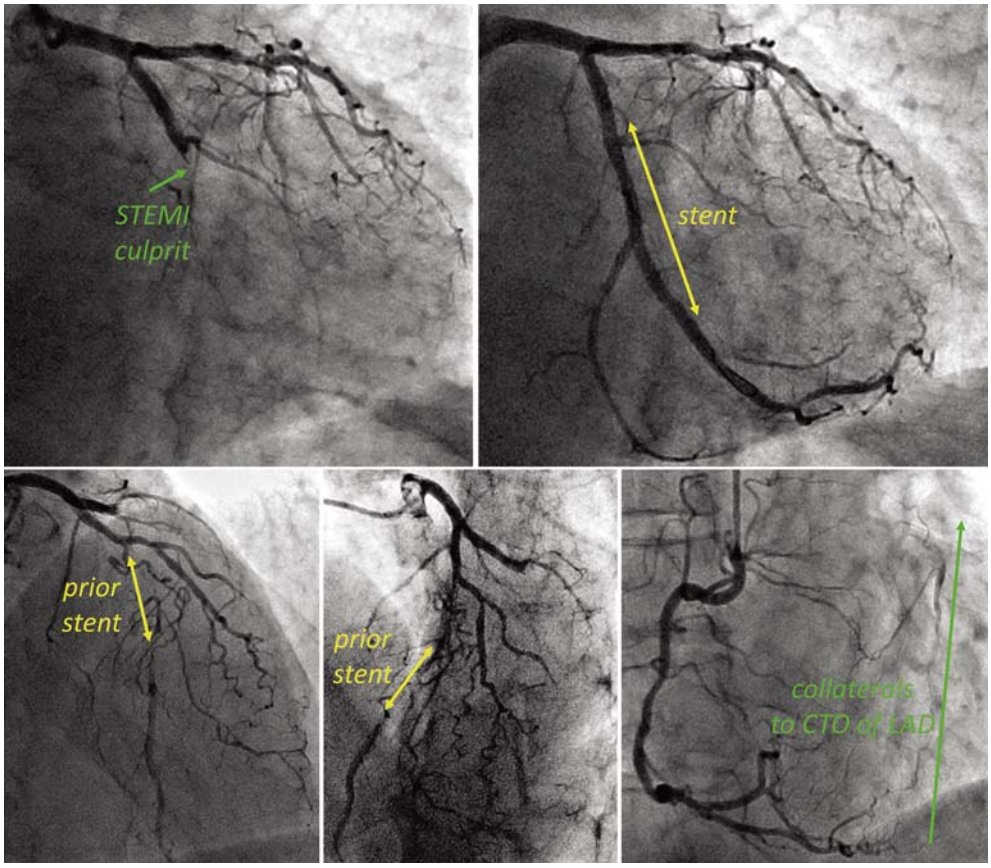

Figure 1 Baseline angiogram.
A 57-year-old man presented with an inferolateral ST-segment elevation myocardial infarction (STEMI) due to an acute occlusion of his left circumflex, rapidly treated by stent placement. His prior stent in the left anterior descending (LAD) artery was found to be a chronic total occlusion (CTO) supplied by both bridging and retrograde collaterals.

family history) before performing two cardiac PET scans about 1 week apart (17). Normal resting flow in this cohort was 0.7 cc/min/g and hyperemic flow reached 2.9 cc/min/g for an absolute coronary flow reserve (CFR) of 4.2－thereby establishing the upper end of the flow continuum.

Some patients exhibit signs and symptoms of clear-cut ischemia during vasodilator imaging, including clinical angina (distinct from the vague chest symptoms often encountered during adenosine or dipyridamole infusion), significant ST-segment changes, and a focal perfusion defect. In our series of almost 4,200 cardiac PET cases, when many or all of these features were present, absolute flow was generally 1 cc/min/g or less and CFR 1.5 or less (18, 19). These low flow bounds demonstrated high diagnostic performance for identifying clinical ischemia. At even lower levels of flow, generally 0.2 cc/min/g (more than 3 standard deviations below normal flow in volunteers), the myocardium either infarcts or hibernates.

Between these two extremes of infarct/ischemia and normal flow exists a wide continuum. Clinical risk falls in continuous fashion when moving from the lowest to highest quartiles of stress flow and absolute CFR, with no gradient observed for resting flow (20). Since stress flow and absolute CFR predict prognosis and associate with ischemia, focusing on either alone neglects important and complementary information. Therefore, we developed the integrative concept of coronary flow capacity (CFC) to synthesize both parameters and locate them along the flow spectrum as detailed earlier (21). Emerging work using both invasive (22) and non-invasive (23) methods to assess CFC has demonstrated its diagnostic and prognostic ability.

Subendocardial versus transmural perfusion

Fundamental animal work from 40 years ago demonstrated that progressive epicardial stenosis reduces downstream myocardial perfusion (24). However, the reduction in flow does not affect all layers of the myocardium equally. As can be seen from the tomographs in that manuscript (especially its Figure 4), the subendocardium experiences a more dramatic and earlier decrease in perfusion compared to the subepicardium. This imbalance arises due to higher compressive forces against the subendocardium from the left ventricular cavity during systole versus the lower pressure against the subepicardium from the pericardial and thoracic spaces (25).

As a physiologic consequence, the subepicardium reper-

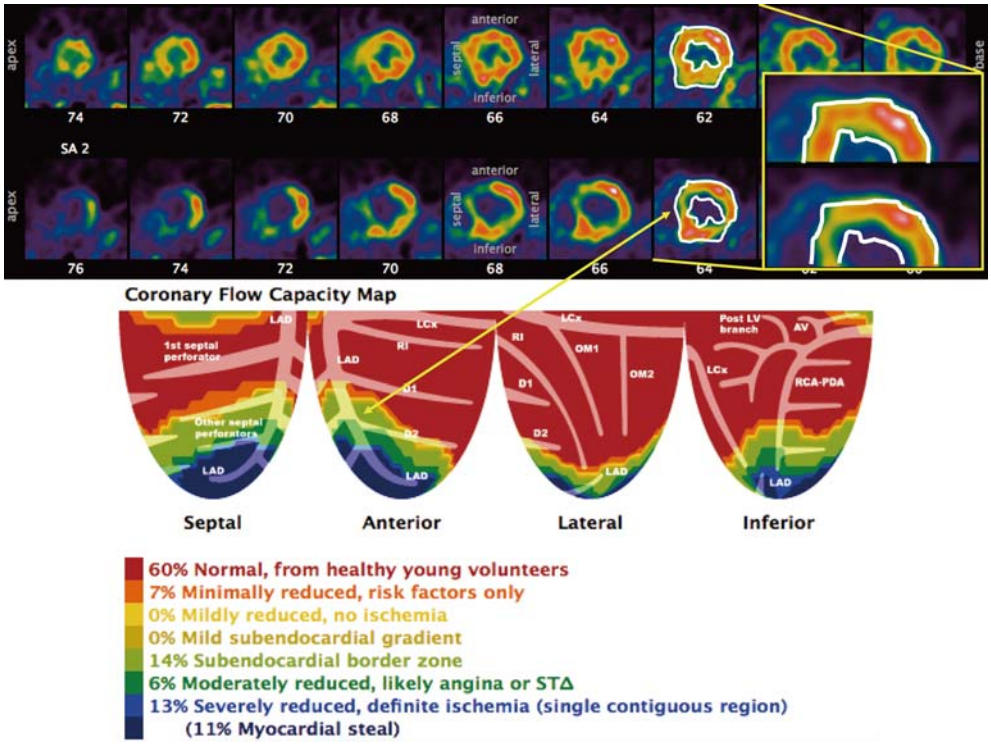

Figure 2　Coronary flow capacity (CFC).

Cardiac positron emission tomography (PET) imaging at rest (top row) and stress (bottom row) revealed a large, almost completely reversible defect in the mid-to-apical anteroseptum corresponding to the known chronic total occlusion of the left anterior descending artery. Quantitative absolute blood flow indicated that 11% of the left ventricle experienced myocardial steal (a decrease in flow during vasodilator stress) with a further 22% ischemic. The borderzone region displayed subendocardial ischemia, as detailed by the inset images.

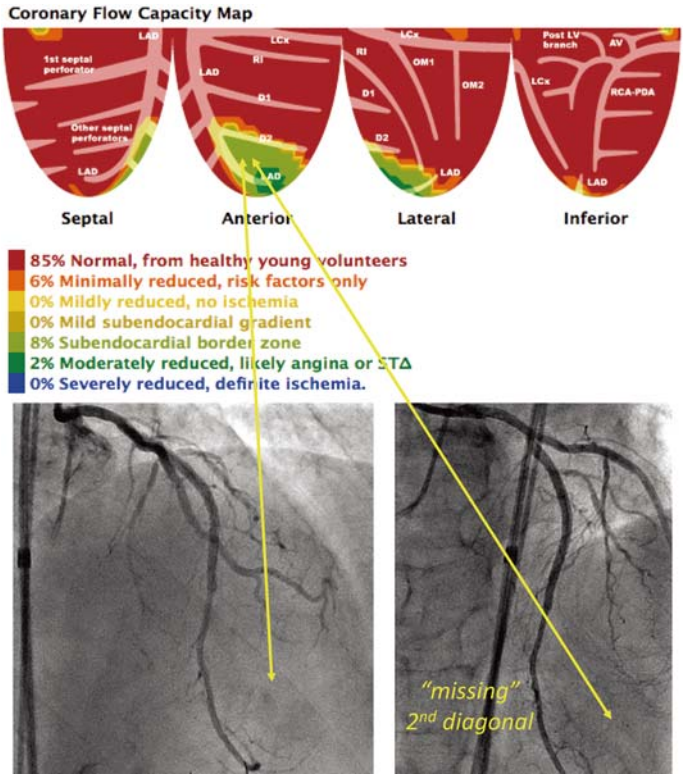

Figure 3　After revascularization.

Successful revascularization of the chronic total occlusion resulted in a vastly improved coronary flow capacity. However, the perfusion map indicates that a second diagonal branch must be flush occluded and not appreciated angiographically. Due to its modest size and severity, further invasive procedures were not pursued.

fuses approximately 20 seconds before the subendocardium following a transient occlusion of an epicardial coronary artery (26). Additionally, microsphere work in animals has shown that “the decrease in subendocardial and increase in subepicardial flow were often associated with normal or even elevated total coronary blood flows so that under the circumstances of these changes, methods that measure only total left ventricular flow … give limited information” (27). Cardiac PET can image subendocardial perfusion (28), although it does not have the axial resolution of magnetic resonance imaging. Emerging work from our group has focused on the relationship between relative stress flow and reduced subendocardial perfusion.

Clinical example

A 57 year-old man with a prior stent several years earlier presented with an ST-segment elevation myocardial infarction. During treatment of the left circumflex culprit, a chronic total occlusion (CTO) of the previously placed left anterior descending stent was noted (Figure 1). Although he returned to running 10 kilometers per day without angina, and his ejection fraction was intact, cardiac PET revealed viable yet ischemic myocardium distal to the CTO with myocardial steal in 11% plus an additional 22% with reduced CFC including a subendocardial borderzone (Figure. 2). After technically successful revascularization of the CTO, the CFC improved dramatically, indicating concurrent physiologic success (Figure 3). This case demonstrates the ability of cardiac PET to resolve a clinical dilemma by providing sophisticated physiologic imaging in a display format ideal for making a revascularization decision and monitoring its effect.

Acknowledgment

None.

Financial support and relationships with industry

NPJ received internal funding from the Weatherhead PET Center for Preventing and Reversing Atherosclerosis; has an institutional licensing and consulting agreement with Boston Scientific for the smart minimum FFR algorithm; received significant institutional research support from St. Jude Medical (CONTRAST, NCT02184117) and Philips Volcano Corporation (DEFINE-FLOW, NCT02328820) for studies using intracoronary pressure and flow sensors; and has a patent pending on diagnostic methods for quantifying aortic stenosis and TAVI physiology.

Conflicts of interest

None.

Reprint requests and correspondence:

Nils P. Johnson, MD, MS

Weatherhead PET Center, McGovern Medical School at UTHealth, 6431 Fannin St., Room MSB 4.256, Houston, TX 77030, USA

E-mail: Nils.Johnson@uth.tmc.edu

References

1. Bing RJ, Hammond MM, Handelsman JC, et al. The measurement of coronary blood flow, oxygen consumption, and efficiency of the left ventricle in man. Am Heart J 1949; 38: 1–24.
2. Gould KL, Schelbert HR, Phelps ME, et al. Noninvasive assessment of coronary stenoses with myocardial perfusion imaging during pharmacologic coronary vasodilatation. V. Detection of 47 percent diameter coronary stenosis with intravenous nitrogen-13 ammonia and emission-computed tomography in intact dogs. Am J Cardiol 1979; 43: 200–8.
3. Schelbert HR, Wisenberg G, Phelps ME, et al. Noninvasive assessment of coronary stenoses by myocardial imaging during pharmacologic coronary vasodilation. VI. Detection of coronary artery disease in human beings with intravenous N-13 ammonia and positron computed tomography. Am J Cardiol 1982; 49: 1197–207.
4. Gould KL, Johnson NP, Bateman TM, et al. Anatomic versus physiologic assessment of coronary artery disease. Role of coronary flow reserve, fractional flow reserve, and positron emission tomography imaging in revascularization decision-making. J Am Coll Cardiol 2013; 62: 1639–53.
5. Patel MR, Peterson ED, Dai D, et al. Low diagnostic yield of elective coronary angiography. N Engl J Med 2010; 362: 886–95.
6. Douglas PS, Pontone G, Hlatky MA, et al. Clinical outcomes of fractional flow reserve by computed tomographic angiography-guided diagnostic strategies vs. usual care in patients with suspected coronary artery disease: the prospective longitudinal trial of FFR (CT): outcome and resource impacts study. Eur Heart J 2015; 36: 3359–67.
7. Desai NR, Bradley SM, Parzynski CS, et al. Appropriate use criteria for coronary revascularization and trends in utilization, patient selection, and appropriateness of percutaneous coronary intervention. JAMA 2015; 314: 2045–53.
8. National Coverage Determination (NCD) for Percutaneous Transluminal Angioplasty (PTA) (20.7). URL https://www.cms. gov/medicare-coverage-database/details/ncd-details. aspx?NCDId=201&ncdver=9&bc=BAABAAAAAAAA, accessed August 16, 2018.
9. Hachamovitch R, Nutter B, Hlatky MA, et al. Patient management after noninvasive cardiac imaging results from SPARC (Study of myocardial perfusion and coronary anatomy imaging roles in coronary artery disease). J Am Coll Cardiol 2012; 59: 462–74.
10. Nakagawa Y, Nakagawa K, Sdringola S, et al. A precise, three-dimensional atlas of myocardial perfusion correlated with coronary arteriographic anatomy. J Nucl Cardiol 2001; 8:

580–90.
11. Pijls NHJ, De Bruyne B. Fractional collateral blood flow. In: Coronary Pressure. Dordrecht, Netherlands: Kluwer Academic Publishers, 1997: 329 (section 12.2).
12. Yoshida K, Mullani N, Gould KL. Coronary flow and flow reserve by PET simplified for clinical applications using rubidium-82 or nitrogen-13-ammonia. J Nucl Med 1996; 37: 1701–12.
13. Kitkungvan D, Johnson NP, Roby AE, et al. Routine clinical quantitative rest stress myocardial perfusion for managing coronary artery disease: clinical relevance of test-retest variability. JACC Cardiovasc Imaging 2017; 10: 565–77.
14. Lautamäki R, George RT, Kitagawa K, et al. Rubidium-82 PET-CT for quantitative assessment of myocardial blood flow: validation in a canine model of coronary artery stenosis. Eur J Nucl Med Mol Imaging 2009; 36: 576–86.
15. Agostini D, Roule V, Nganoa C, et al. First validation of myocardial flow reserve assessed by dynamic ^{99m}Tc-sestamibi CZT-SPECT camera: head to head comparison with ^{15}O-water PET and fractional flow reserve in patients with suspected coronary artery disease. The WATERDAY study. Eur J Nucl Med Mol Imaging 2018; 45: 1079–90.
16. Wells RG, Marvin B, Poirier M, et al. Optimization of SPECT measurement of myocardial blood flow with corrections for attenuation, motion, and blood binding compared with PET. J Nucl Med 2017; 58: 2013–9.
17. Sdringola S, Johnson NP, Kirkeeide RL, et al. Impact of unexpected factors on quantitative myocardial perfusion and coronary flow reserve in young, asymptomatic volunteers. JACC Cardiovasc Imaging 2011; 4: 402–12.
18. Johnson NP, Gould KL. Physiological basis for angina and ST-segment change PET-verified thresholds of quantitative stress myocardial perfusion and coronary flow reserve. JACC Cardiovasc Imaging 2011; 4: 990–8.
19. Added Screen Displays For FDA Cleared HeartSee Cardiac P.E.T Processing Software K143664. URL https: //www. accessdata. fda. gov/scripts/cdrh/cfdocs/cfpmn/pmn. cfm? ID = K171303, accessed August 16, 2018.
20. Wang L, Jerosch-Herold M, Jacobs DR Jr, et al. Coronary risk factors and myocardial perfusion in asymptomatic adults: the Multi-Ethnic Study of Atherosclerosis (MESA). J Am Coll Cardiol 2006; 47: 565–72.
21. Johnson NP, Gould KL. Integrating noninvasive absolute flow, coronary flow reserve, and ischemic thresholds into a comprehensive map of physiological severity. JACC Cardiovasc Imaging 2012; 5: 430–40.
22. van de Hoef TP, Echavarría-Pinto M, van Lavieren MA, et al. Diagnostic and prognostic implications of coronary flow capacity: a comprehensive cross-modality physiological concept in ischemic heart disease. JACC Cardiovasc Interv 2015; 8: 1670–80.
23. Gould KL, Johnson NP, Roby AE, et al. Regional artery specific thresholds of quantitative myocardial perfusion by PET associated with reduced MI and death after revascularization in stable CAD. J Nucl Med 2019; 60: 410–7.
24. Gould KL. Assessment of coronary stenoses with myocardial perfusion imaging during pharmacologic coronary vasodilatation. IV. Limits of detection of stenosis with idealized experimental cross-sectional myocardial imaging. Am J Cardiol 1978; 42: 761–8.
25. Duncker DJ, Bache RJ. Regulation of coronary blood flow during exercise. Physiol Rev 2008; 88: 1009–86.
26. Downey HF, Crystal GJ, Bashour FA. Asynchronous transmural perfusion during coronary reactive hyperaemia. Cardiovasc Res 1983; 17: 200–6.
27. Buckberg GD, Fixler DE, Archie JP, et al. Experimental subendocardial ischemia in dogs with normal coronary arteries. Circ Res 1972; 30: 67–81.
28. Danad I, Raijmakers PG, Harms HJ, et al. Impact of anatomical and functional severity of coronary atherosclerotic plaques on the transmural perfusion gradient: a [^{15}O] H_2O PET study. Eur Heart J 2014; 35: 2094–105.